EXCITATION OF GIANT MONOPOLE AND QUADRUPOLE RESONANCES

H. OGATA, T. YAMAGATA[+], M. TANAKA[++], S. KISHIMOTO[+], K. YUASA[+], K. IWAMOTO[+],
B. SAEKI[+], T. FUKUDA[*], I. MIURA and M. INOUE

Research Center for Nuclear Physics, Osaka University, Suita, Osaka

[+] Department of Physics, Konan University

[++] Kobe Tokiwa Junior College

[*] Department of Physics, Osaka University

ABSTRACT

Recent studies on the giant monopole resonance (GMR) and the giant quadrupole resonance (GQR) in ^{144}Sm and ^{208}Pb using the α-scattering performed at RCNP are summarized. The observed angular range covered 1.6°∼7.° with a coupled system of a dipole and a triplet quadrupole magnet. The incident energy was changed from 84 to 119 MeV. The resonance shapes and energy-weighted sum-rule strengths of the GMR and the GQR were reliably deduced as a function of incident energy. The quadrupole strength of ∼20% was found in the GMR region. The observed excitation function of the GMR was compared with the DWBA calculation, in which the Satchler's Version I was used as a form factor representing the compressional motion of the nucleus. It was found that the experimental excitation function of the GMR shows steeper decrease as lowering the incident energy than the DWBA prediction whereas that of the GQR is successfully described by the DWBA. This suggests that examination of the model describing the GMR is necessary.

1. INTRODUCTION

The giant monopole resonance (GMR) has received considerable interest in recent years in connection with the compressibility of nuclear matter[1] which is unobtainable in other ways. The conclusive evidence of the GMR was obtained in medium and heavy mass nuclei by measurement of inelastic hadron scattering at extremely forward angles[2-6]. It was found that the GMR occurs at an excitation energy of $E_x \sim 80A^{-1/3}$ MeV, very closed to the giant quadrupole resonance (GQR) at $E_x \sim 63A^{-1/3}$ MeV. However, the previously observed shapes and strengths of the GMR have been rather qualitative. The angular distributions of the GMR were not so well reproduced by the theoretical calculations as those of the neighboring GQR. This feature suggests that the shapes and strengths of the GMR were not correctly evaluated and that the reexamination

of those quantities not only for the GMR but also for the neighboring GQR is necessary.

Several models for the DWBA calculation of the excitation of the GMR[7,8] were employed in the deduction of transition strength. However, the validity of these DWBA predictions on the GMR has not been examined experimentally due to the absence of the collective 0^+ levels at low-lying excitation region. The measurement of the excitaiton function is effective in investigating the models for the GMR excitation. Recently, the excitation functions of the GMR and GQR in ^{208}Pb were observed in the inelastic scattering of α-particles at E_α=100-172 MeV[9]. However, since the observed angle was restricted only to the third maxima of the angular distributions for the GMR in the above work, the excitation of the GMR was less pronounced. It seems more desirable to perform measurement on the excitation functions of the GMR in the wider angular range including the extremely forward angles. Going to the lower incident energies it is quite important to carry out the measurement at extremely forward angles, because a steeper fall down in the cross section of the GMR than that of the neighboring GQR is expected as decreasing incident energy and the deduction of the precise value of the strength for the GMR becomes more difficult.

It is the aim of the present paper to describe the measurement of the resonance shape, energy-weighted sum-rule (EWSR) strengths and to discuss the excitation function of the GMR in comparison with the GQR. We carried out the measurement of inelastic scattering of α-particles on ^{144}Sm and ^{208}Pb with incident energies from 84 to 119 MeV at an angular range of 1.6° to 7° in the laboratory system. The incident energy range in the present work covers the energy corresponding to the nuclear sound velocity (v/c∿0.2)[1]. It would be interesting to observe whether an anomaly occurs at this energy or not in the excitation function for the GMR.

2. EXPERIMENTAL PROCEDURES

As well known, the GMR has distinguishable cross sections from the neighboring GQR only at extremely forward angles. However, measurements in such an angular region are very difficult as stressed by many authors[2,3,10]. At RCNP, detection of the scattered particles at those angles is carried out by a coupled system of a triplet quadrupole and a dipole magnet[11]. The former functions as a momentum filter to reject an enomous number of elastically

scattered particles, and the latter as a swinger magnet to measure an angular distribution of scattered particles. The detection system is schematically shown in Fig. 1. The quadrupole magnet is placed down-stream of a 1-m scattering chamber, and a stack of silicon detectors with a total thicknesses of 7-mm is set at the symmetric position with respect to the triplet. The dipole
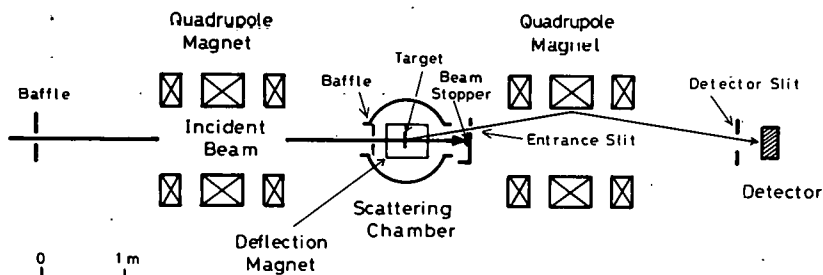

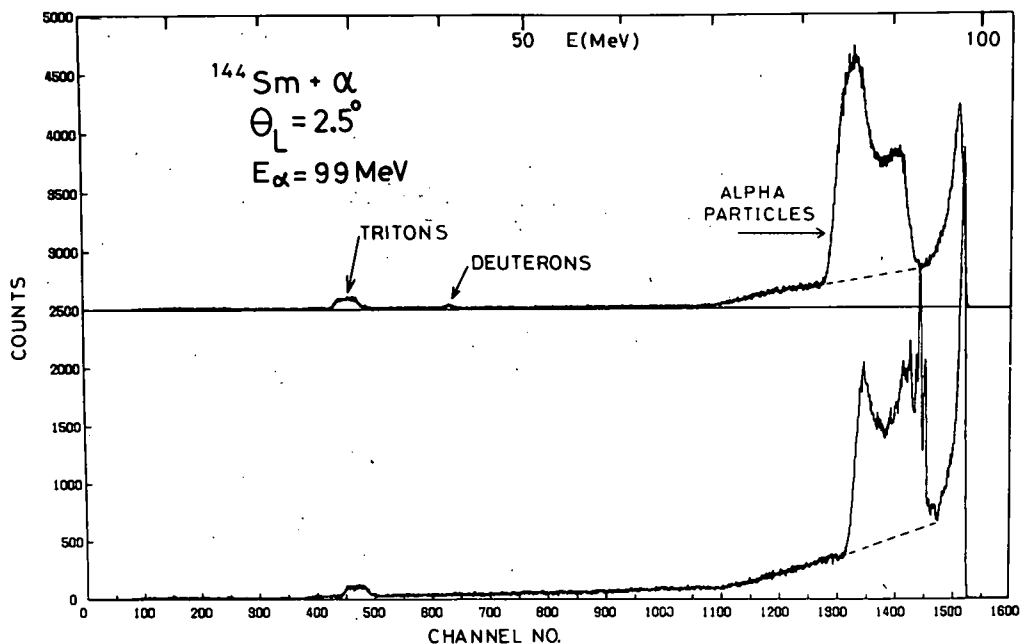Fig. 1. Schematic drawing of the experimental setup.

Fig. 2. Examples of raw energy spectra obtained by the quadrupole magnet system.

magnet is mounted in the scattering chamber in such a way that the target is positioned at its center.

Incident beam extracted from the AVF cyclotron at RCNP is directed through focussing elements into the scattering chamber. Various beam cleaning baffles are inserted in the beam line to minimize the beam halo. Beam transportation system is operated so that any baffles should not cut into the main beam. At the 4.5-m upstream of the target the beam is focussed on a 4-mm aperture baffle which is used as a filter of the impurity beam components. After bombarding the target, the beam is stopped by a graphite beam stopper at the exit of the chamber. The scattered particles are focussed on the detector through the entrance and the detector slit by the quadrupole magnet.

Examples of the energy spectra obtained by this system are shown in Fig. 2; particles emitted from the ^{144}Sm + α reaction at an incident energy of 99 MeV and a laboratory angle of 2.5 degree are detected. Alpha, deuteron and triton groups are separately seen in the figure. The two spectra in the figure are obtained with slightly different settings of the field of the quadrupole magnet. Background lying under the α-particle spectrum is mainly due to the scattered particles from the entrance slit, and can be easily
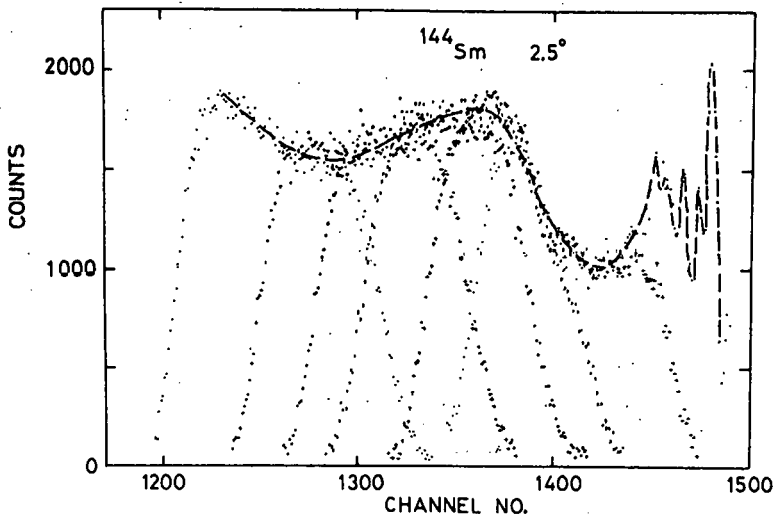

Fig. 3. Whole energy spectrum of the giant resonance region obtained by six measurements with different settings of the quadrupole field.

identified as shown by a broken line under the true inelastically scattered
α-particle spectrum. From the widths in the α-particle spectra, it can be seen
that the spectrometer has a momentum range of flat response of about 3%.

In order to obtain the whole energy spectrum over the region of interest,
several measurements are carried out with various settings of the quadrupole
field ensuring that each spectrum has sufficient overlapping regions with those
of neighboring ones, as typically shown in Fig. 3. In the resultant spectrum
displayed in a dashed line, the giant resonance structure as well as low-lying
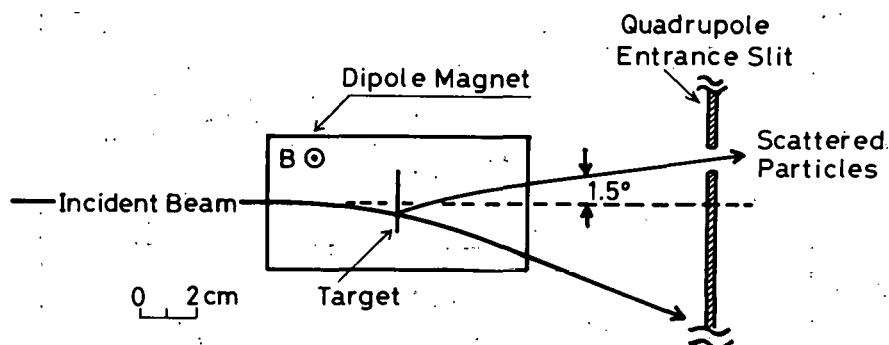discrete states are clearly observed.

Fig. 4. Schematic drawing of the angular distribution measurement with a
dipole magnet.

Fig. 4 shows how the angular distributions are measured by using the
dipole magnet. When the dipole is not excited, scattered particles are detect-
ed at 1.5°. When excited, the incident beam as well as the scattered particles
are vertically deflected. Therefore, the scattering angles of particles
entering the slit can be changed by the field strength of the dipole magnet.
An aperture of the entrance slit is so selected that an angular resolution of
0.5° is given. The calibration of the deflection angle and the effective solid
angle of the system was done by comparing the angular distributions of elastic
and inelastic scattering from ^{144}Sm, ^{208}Pb and ^{12}C observed by this quadrupole
system with that observed by a monitor counter which is vertically movable in
the scattering chamber.

In the present experiment, measurements were done for ^{144}Sm at 84, 99 and
109 MeV incident energies and for ^{208}Pb at 84 and 119 MeV, respectively.
Target thicknesses were 4.0 mg/cm^2 for ^{144}Sm and 6.9 mg/cm^2 for ^{208}Pb.

Fig. 5 shows energy spectra of the inelastically scattered α-particles
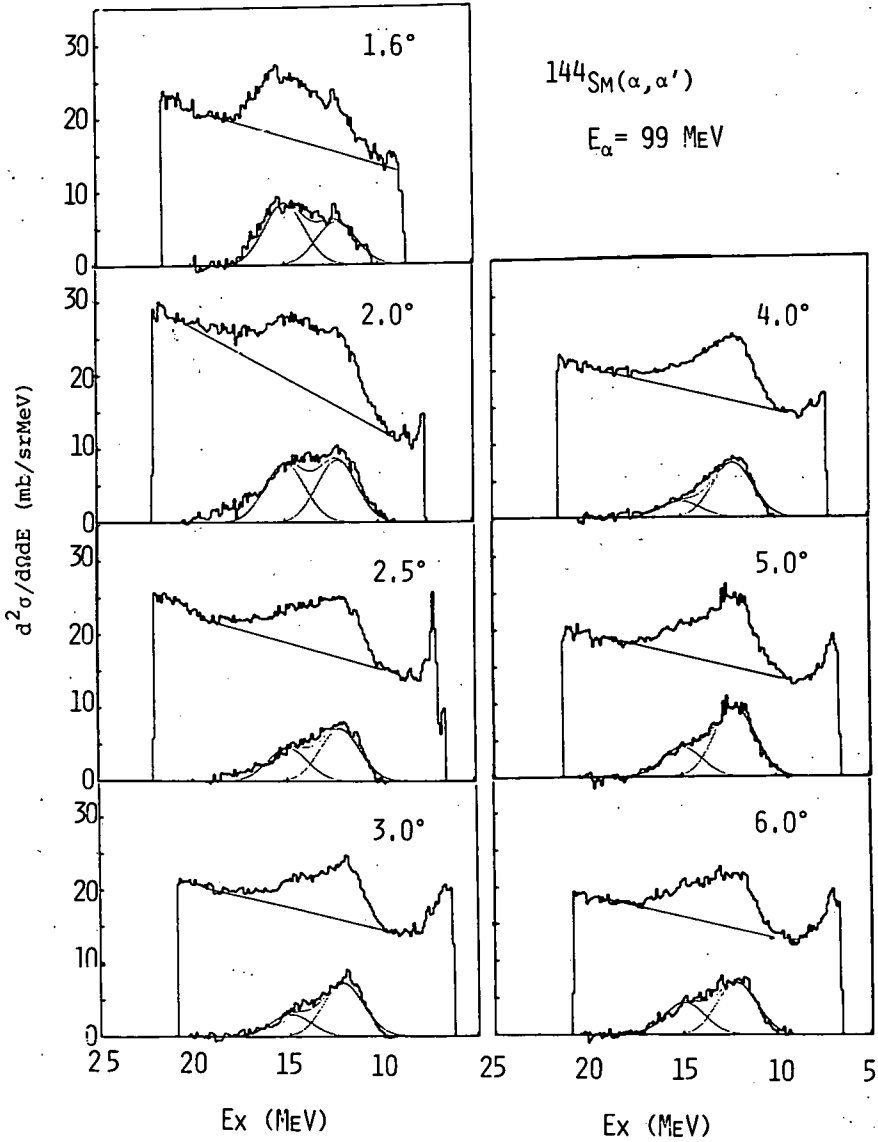

Fig. 5.   Energy spectra of inelastically scattered α-particles from ^{144}Sm at 99 MeV.   The giant resonances are seen on the continuum.   Sabtracted spectra assuming the shape of underlying continuum as linear function (solid lines) are shown under the original.   Decompositions of the giant resonances into two gaussians are also shown by thin lines.

from ^{144}Sm at 99 MeV. In each spectrum, an asymmetric resonance structure can be observed on underlying continuum. At E_x=12.5 MeV, the well known GQR[2,12] is seen to be excited at every scattering angle. At forward angles, another resonance is discernible to be excited at 15.2 MeV. This gives a strong evidence for the excitation of the GMR[2]. Under each original spectrum, is shown only the resonance part of the spectrum after subtraction of the underlying continuum assuming a straight line as indicated in the upper spectra. In Fig. 6, the resonance parts of the spectra for ^{144}Sm(α,α') reactions at 109 and 84 MeV are summarized after subraction of underlying continuum. It is noted that at 109 MeV, the 15.2 MeV resonance is found much more strongly excited than at 99 MeV, especially at forward angles smaller than 2.5 deg. However, at the lowest incident energy of 84 MeV, the 15.2 MeV resonance is slightly excited only at the most forward angles ($\theta_L \lesssim 2.5°$).

In Fig. 7, are shown spectra for ^{208}Pb after subraction of the continuum at 119 and 84 MeV. At the incident energy of 119 MeV two resonances are clearly seen; the 11.0 MeV resonance[2,3,12] is already known as the GQR and 13.5 MeV resonance is sharply pronounced at forward angles. Again in ^{208}Pb, a powerful evidence for the GMR at 13.5 MeV have been obtained. However, in the left hand side of the figure, the spectra at an incident energy of 84 MeV are peaked only at 11.0 MeV, and have similar shapes to each other. At the first glance, no evidence for the GMR excitation can be obtained.

In the Fig. 6 are indicated the kinematical limits of the break-up α-particles from (α,^{5}Li) and (α,^{5}He) reactions. Their contributions were estimated[13] to be small (less than 1mb/sr MeV) and was found to have no influence on the evaluation of the cross section of the GMR.

In order to obtain the angular distributions of these resonances in ^{144}Sm and ^{208}Pb, the energy spectrum is decomposed into two peaks with gaussian shapes after subtracting underlying continuum. In this procedure, sharp peaks due to the discrete levels of the target and contaminative nuclei are also subtracted. The results are shown in the spectra as shown by thin lines in Figs. 5-7. Fig. 8 shows the angular distributions of these resonance components in ^{144}Sm at 109, 99 and 84 MeV. Error-bars are mainly due to the uncertainty in procedures of the continuum subtraction and the decomposition into two components. It should be noted that at higher incident energies (109 MeV and 99 MeV) the angular distributions of the two components are different
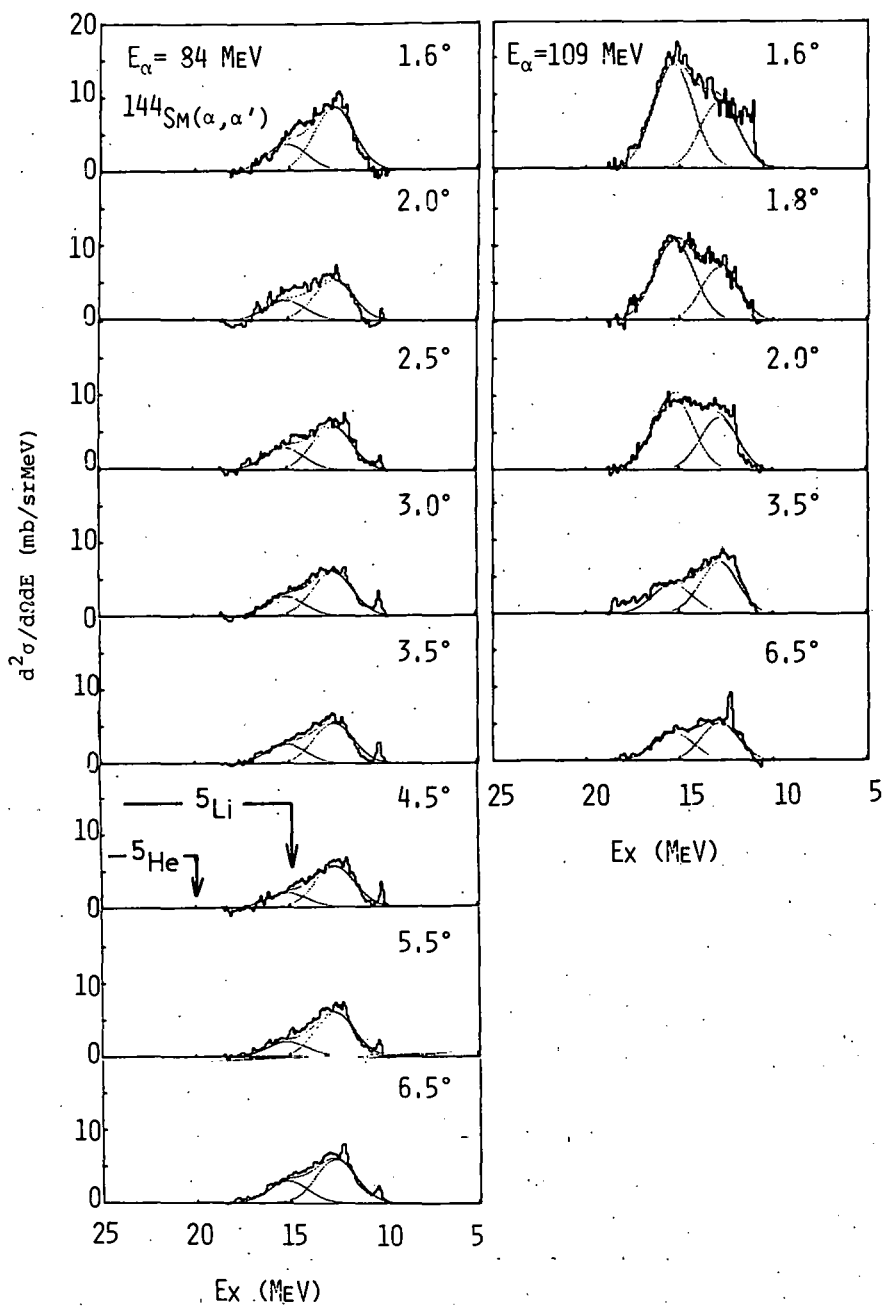
Fig. 6. Resonance spectra of ^{144}Sm at 84 and 109 MeV after subtraction of underlying continuum. Kinematical limit of α-particles from (α,^{5}Li) and (α,^{5}He) reactions are shown by arrows. See caption of Fig. 5.
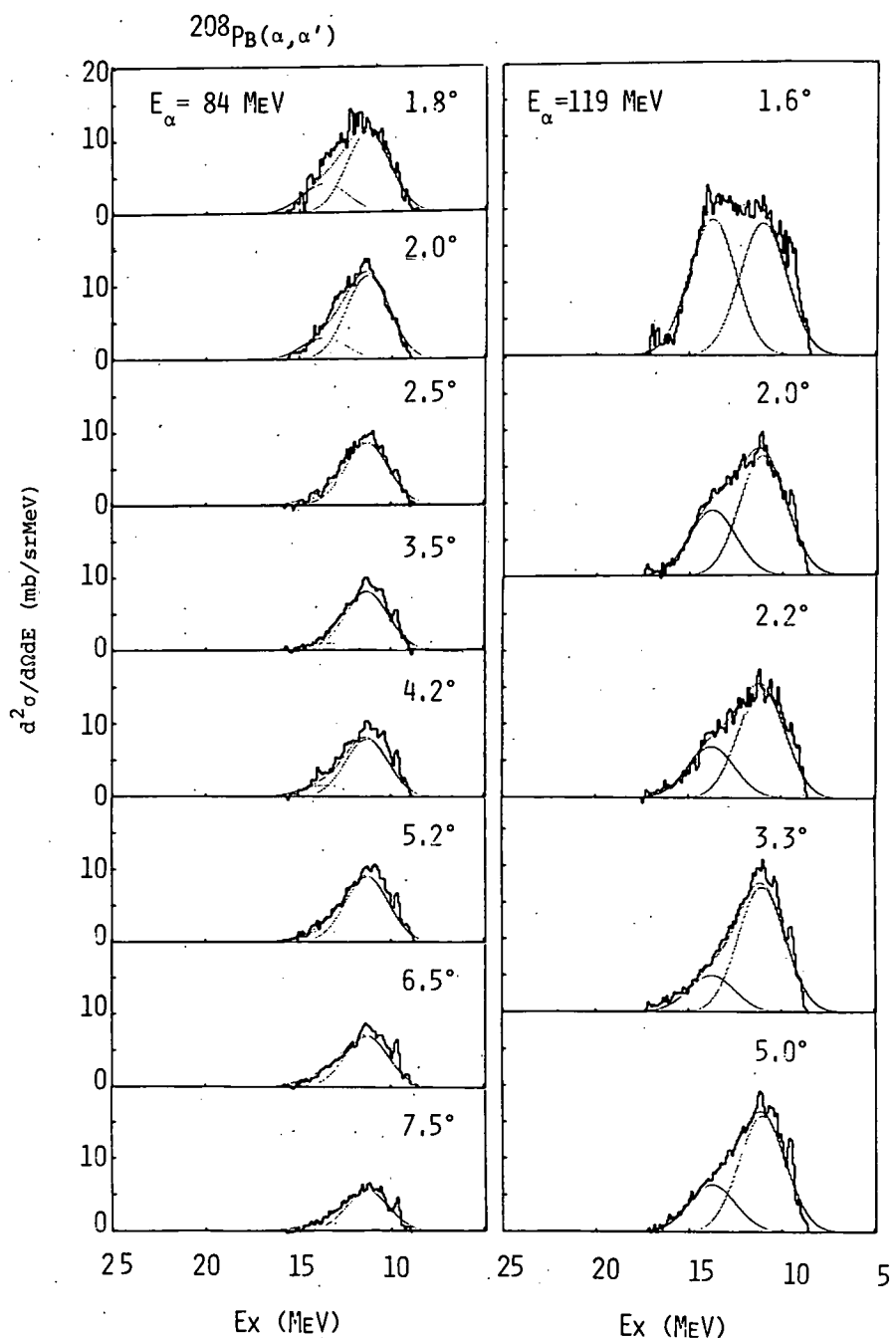
Fig. 7. Resonance spectra of ^{208}Pb at 84 MeV and 119 MeV after subtraction of underlying continuum. See caption of Fig. 5.

from each other; the angular distribution for 12.5 MeV component is relatively flat, whereas that for 15.2 MeV is sharply pronounced at the forward angles. At the lowest incident energy of 84 MeV, both resonances have very similar
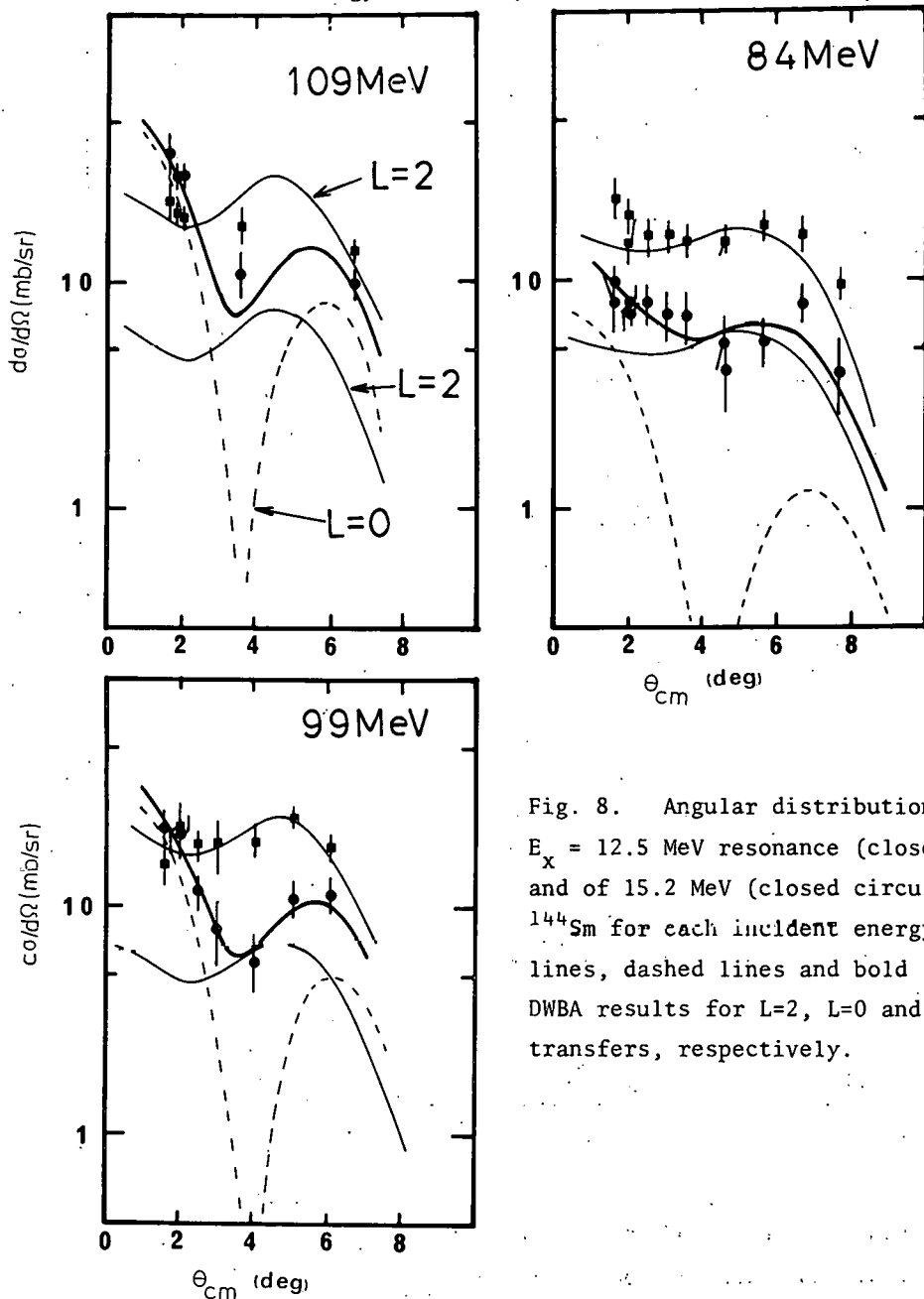

Fig. 8. Angular distributions of E_x = 12.5 MeV resonance (closed squares) and of 15.2 MeV (closed circules) in ^{144}Sm for each incident energy. Thin lines, dashed lines and bold lines are DWBA results for L=2, L=0 and L=0+2 transfers, respectively.

anglular distributions to one another. In Fig. 9, are shown the angular distributions for the two components in ^{208}Pb at 119 and 84 MeV, respectively. Again, the angular distributions at 119 MeV and 84 MeV display similar behaviors to those as described at 109 MeV and 84 MeV in the ^{144}Sm case, respectively.

These angular distributions were analysed in terms of the DWBA[14]. The optical potential parameters taken from ref. 12 were used energy independently. The form factor for excitation of the GQR was of a collective type. For excitation of the GMR, the form factor of Satchler's Version I, representing the compressional motion of nucleus, were used[7]. From Figs. 8 and 9, the angular distributions for the lower resonance components at 12.5 MeV in ^{144}Sm and 11.0 MeV in ^{208}Pb are seen to be well fitted by the DWBA calculations for L=2 transfers. On the other hand, those for the higher components at 15.2 MeV in ^{144}Sm and at 13.5 MeV in ^{208}Pb are well fitted by the DWBA calculations for L=0 transfer at the highest incident energies except at the region of the first minima, but poorly fitted at the lowest incident energies. The angular
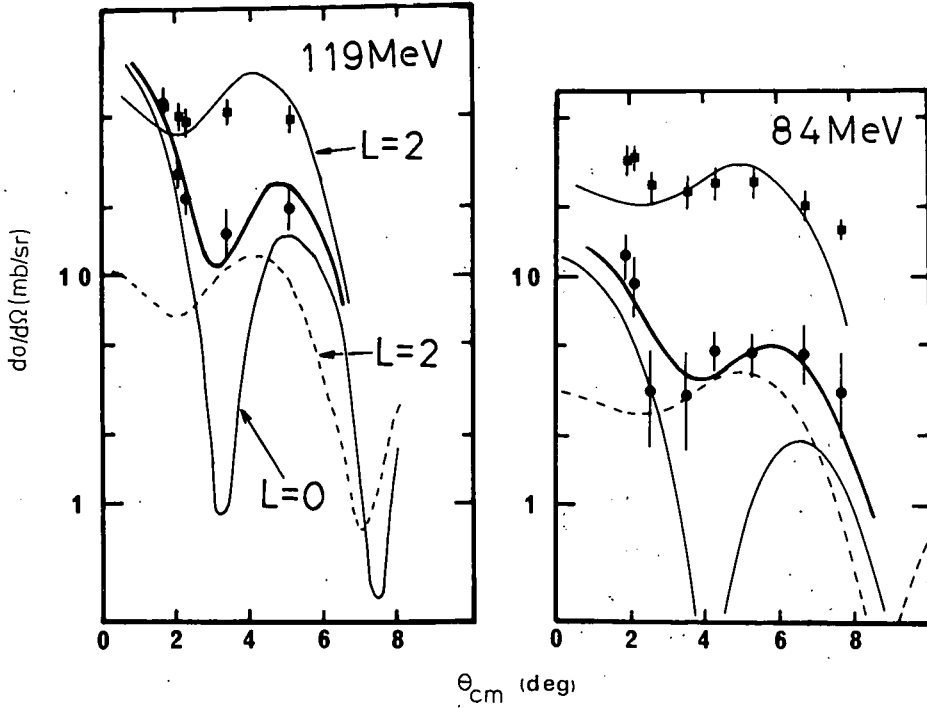

Fig. 9. Angular distributions of E_x = 11.0 MeV resonance (closed squares) and of 13.5 MeV (closed circules) in ^{208}Pb. Thin lines, dashed line and bold line are DWBA results for L=2, L=0 and L=0+2 transfer, respectively.

distributions of the high energy components rather resemble to that of the low
energy component (L=2). There fact suggests that an additional component of
L=2 transfer exists in the higher excitation component and the observed angular
distributions of the high energy component are well fitted with a combination
of L=0 and 2 transfers at each incident energy as shown by the bold lines in
Fig. 8 and 9.

In Table I, are summarized the observed excitation energies and EWSR
strengths for the GQR and the GMR in ^{144}Sm and ^{208}Pb together with other
results. In Fig. 10, the EWSR strengths thus obtained are displayed as a
function of the incident energy.

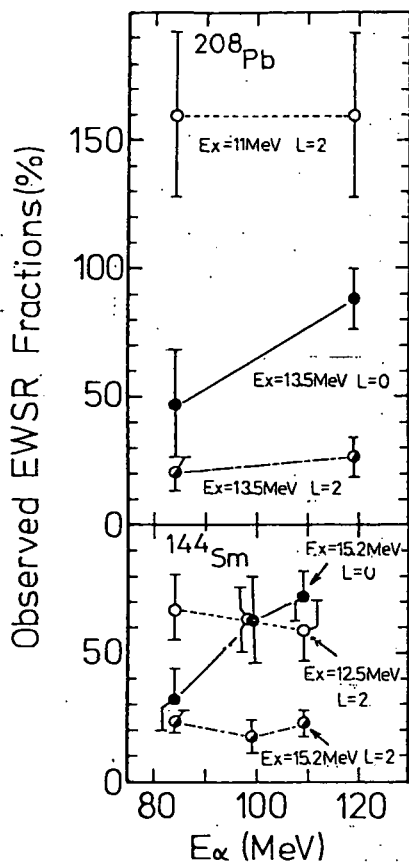Fig. 10. Incident energy dependence of experimentally deduced EWSR strength for ^{144}Sm and ^{208}Pb.

Table I.   Parameters for GQR and GMR

Nucleus	E_i (MeV)	GMR			GQR[b]		
		E_x (MeV)	Width(MeV)	EWSR(%)	E_x (MeV)	Width(MeV)	EWSR(%)
^{144}Sm	84	14.9	2.5	32.1±12	12.4	3.6	89.9±14.0
	99	15.3	2.5	63.1±17.4	12.5	3.4	80.5±14.8
	109	15.1	2.5	72.5±9.4	12.6	3.3	81.8±13.4
		15.2	2.5		12.5	3.4	
	129[a]	14.8±0.3	2.9±0.2	85±20	12.4±0.2	2.3±0.3	100±25
^{208}Pb	84	13.4	2.9	47.0±21.5	11.0	2.8	181±33.5 [154.3±33.5(L=2) + 20.1±6.7(L=4)]
	119	13.6	3.0	88.6±12.1	10.9	3.0	187.8±33.5 [161.0±33.5(L=2) + 20.1±6.7(L=4)]
		13.5	3.0		11.0	2.9	
	127[a]	13.7±0.4	3.0±0.5	90±20	11.0±0.2	2.7±0.3	105±25

[a] Ref. 4.   [b] Including the contribution in the GMR region.

4. DISCUSSIONS

As seen in Fig. 10 and Table I, the main parts of the strengths of the EWSR for the GQR are exhausted by the lower resonance component for both ^{144}Sm and ^{208}Pb. However, there still remain the quadrupole strenghs of about ~ 20% in the higher component for ^{144}Sm and ^{208}Pb, respectively. This shows that the GQR has a tail toward the GMR and has not a symmetric gaussian shape but an asymmetric shape. The intrinsic shape of the GQR can be directly seen at the angles where contributions from the GMR reach the minima; for examples, spectra at 4.1° of 99 MeV for ^{144}Sm and 3.2° of 119 MeV for ^{208}Pb show the shapes of the GQR. As a result, deduced widths of the GQR in the present work are considerably larger than previously observed[2,4]. Including the contributions from higher components, the EWSR strengths for the GQR are 80% and 180% for ^{144}Sm and ^{208}Pb, respectively. In connection to the large EWSR strength for the GQR in ^{208}Pb, experimental results were better fitted by considering the admixture of L=4 transfer, as seen in Fig. 11. Then the lower component at 11 MeV may consist of two components with 107% E2 and 20% E4 strengths. In this

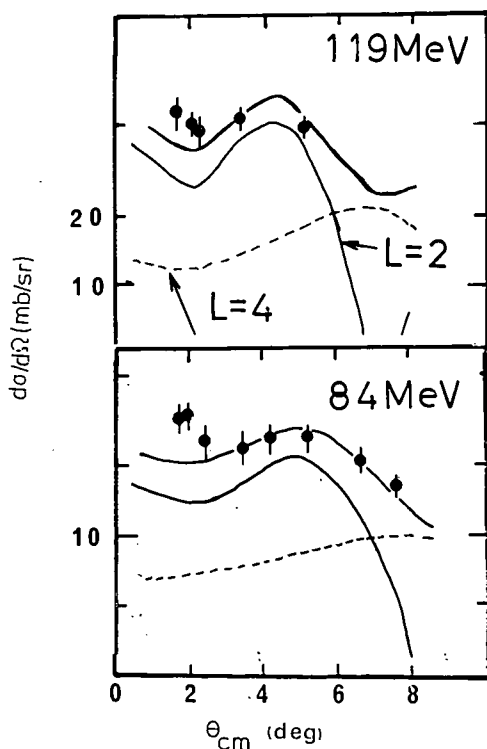Fig. 11. DWBA fitting for the E_x = 11 MeV resonance in ^{208}Pb by mixing L=2 and L=4 transfers.

region, the existence of E4 component of about 20% of EWSR is predicted by various theories such as an RPA calculation done by Speth[15]. The present result is in good agreement with these predictions.

As shown in Fig. 10, it should be noticed that the experimentally deduced EWSR strengths of the GMR decrease prominent from 72% at 109 MeV down to 32% at 84 MeV for ^{144}Sm and from 88% at 119 MeV to 47% at 84 MeV for ^{208}Pb. This unexpected behavior makes a remarkable contrast with the behavior for the GQR, which shows nearly a constant EWSR strength over the same range of the incident energy. This result is more intuitively seen in Fig. 12, where the energy spectra of ^{144}Sm and ^{208}Pb are again presented at fixed angles at different incident energies. The dotted lines in the spectra at E =84 MeV are the DWBA predictions using the strengths obtained at higher incident energies (109 MeV for ^{144}Sm and 119 MeV for ^{208}Pb). In order to test the effect of the distorted waves, a different set[16] of the optical potentials was applied for the DWBA
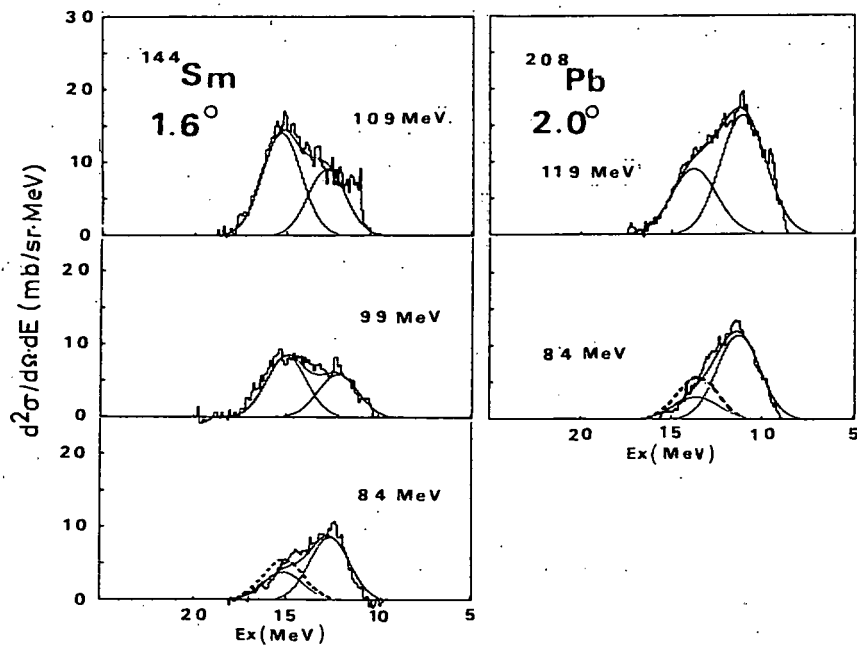

Fig. 12. Giant resonance spectra at fixed angles of 1.6° and 2.6° for ^{144}Sm and ^{208}Pb, respectively, at different incident energies. Dotted lines in the spectra at the lowest incident energy show results of the DWBA predictions using the strengths obtained at higher incident energies (^{144}Sm at 109 MeV and ^{208}Pb at 119 MeV).

calculation. However, this situation was not changed much, although absolute values in the EWSR strengths were somewhat changed. Therefore, these results suggest that the model of the form factors used in the present calculation are not good enough to provide the correct dependence of the GMR excitation on the incident energy.

The steep decrease in the GMR cross section mentioned above may indicate that the excitation of the GMR should be studied from a different point of view. It would be interesting that the velocity of 84 MeV α-particles at the nuclear surface of the target is closed to the nuclear sound velocity derived from the nuclear compressibility modulus[1].

5. CONCLUSION

In conclusion, we have studied the excitations of the GMR and the GQR in ^{144}Sm and ^{208}Pb, changing the incident α-particle energy. The experimentally deduced EWSR strengths for the GMR show a strong dependence on the incident energy, no matter what the EWSR strength in itself should not depend on the incident energy. This situation could not be explained by the conventional DWBA calculation, using a form factor based on the model of compressional motion of the nucleus for the GMR[7]. This indicates that the examination of the model for the GMR is necessary. Farther analysis of the present results with other types of form factors is under progress. Measurements of the incident energy dependence of the cross section have proved very useful to investigate other aspects of the giant resonances which are not obtained from the measurement of angular distributions alone.

Lastly, for either ^{144}Sm and ^{208}Pb, the shape of the GQR is found asymmetric and to have a tail toward the GMR. It is stressed that this tail should be carefully considered in detailed studies on the GMR and the GQR.

REFERENCES

1. J.P. Blaizot, D. Gogny and B. Grammaticos, Nucl. Phys. A265 (1976) 315.
2. D.H. Youngblood, C.M. Rozsa, J.M. Moss, D.R. Brown and J.D. Bronson, Phys. Rev. Lett. 39 (1977) 1188.
3. M. Buenerd, C. Bonhomme, D. Lebrun, P. Martin, J. Chauvin, G. Duhamel, G. Perrin and P. de Saintignon, Phys. Lett. 84B (1979) 305.
4. D.H. Youngblood, in Proceedings of Giant Multipole Resonance Topical Conference, Oak Ridge, 1979.
5. T. Yamagata, M. Tanaka, T. Fukuda, S. Kishimoto, K. Yuasa, B. Saeki, K. Iwamoto, I. Miura and H. Ogata, ibid.

6. N. Marty, A. Willis, M. Morlet, R. Frascaria, V. Comparat and P. Kitching, ibid.

7. G.R. Satchler, Part. Nucl. $\underline{5}$ (1973) 105.

8. H.P. Morsch and P. Decowski, Phys. Lett. $\underline{82B}$ (1979) 1.

9. H.P. Morsch, M. Rogge, P. Turek, C. Sükösd and C. Mayer-Böricke, Phys. Rev. $\underline{C20}$ (1979) 1600.

10. T. Yamagata, K. Iwamoto, S. Kishimoto, B. Saeki, K. Yuasa, M. Tanaka, T. Fukuda, K. Okada, I. Miura, M. Inoue and H. Ogata, Phys. Rev. Lett. $\underline{40}$ (1978) 1628.

11. T. Yamagata, M. Tanaka, S. Kishimoto, K. Iwamoto, B. Saeki, K. Yuasa, T. Fukuda, I. Miura, M. Inoue and H. Ogata, RCNP Annual Report 1978, P. 168.

12. D.H. Youngblood, J.M. Moss, C.M. Rozsa, J.D. Bronson, A.D. Bacher and D.R. Brown, Phys. Rev. $\underline{C13}$ (1976) 994.

13. D.R. Brown, J.M. Moss, C.M. Rozsa, D.H. Youngblood and J.D. Bronson, Nucl. Phys. $\underline{A313}$ (1979) 157.

14. DWBA calculations were performed using a code "DWUCK" programmed by P.D. Kunz.

15. J. Speth, J.S. Dehesa, A. Faessler, V.A. Madsen, G.A. Rinker and J. Wambach, J. Phys. Soc. Jpn $\underline{44}$ (1978) Suppl. 213.

16. D.A. Goldberg, S.M. Smith, H.G. Pugh, P.G. Roos and N.S. Wall, Phys. Rev. $\underline{C7}$ (1973) 1938.